

The Coupling Method with the Natural Boundary Reduction on an Ellipse for Exterior Anisotropic Problems ¹

Quan Zheng², Jing Wang² and Jing-ya Li²

Abstract: This paper investigates the coupling method of the finite element and the natural boundary element using an elliptic artificial boundary for solving exterior anisotropic problems, and obtains a new error estimate that depends on the mesh size, the location of the elliptic artificial boundary, the number of terms after truncating from the infinite series in the integral. Numerical examples are presented to demonstrate the effectiveness and the properties of this method.

Keywords: Exterior anisotropic problem, coupling method, elliptic artificial boundary, natural boundary reduction, error estimate.

1 Introduction

In practical applications, many scientific and engineering computing problems, such as the radiation and diffraction of electromagnetic waves, the fluid flow around obstacles, etc., often come down to boundary value problems of partial differential equations in unbounded domains. It has focused great attention for the numerical solution of this kind of problems to overcome the infinity of domains efficiently and obtain the appropriate error estimate. Therefore, a lot of methods were proposed in recent decades [Enquist and Majda (1977); Johnson and Nedelec (1980); Feng (1983); Givoli (1992); Yu (2002); Ying (2006); Delfim (2008); Yu and Huang (2008); Koyama (2009)].

Based on the natural boundary reduction, the natural boundary integral method was suggested by Feng and Yu. It can be coupled directly and naturally with the finite element method by using the same variational principle, where the natural boundary integral equation is the exact, non-reflective and nonlocal artificial boundary condition. This coupling method leads to a symmetric and coercive bilinear form

¹ Supported in part by Natural Science Foundation of Beijing (No. 1072009).

² College of Sciences, North China University of Technology, Beijing, P.R. of China.

and is called the natural coupling method of FEM and BEM [see Feng (1983); Feng and Yu (1983); Yu (2002)]. Since this exact artificial boundary condition is just the Dirichlet to Neumann mapping on the artificial boundary, this method is also called the DtN method [Keller and Givoli (1989)]. This coupling method not only enables the natural boundary element method to overcome the limitation of domain shape, but also enables the classical finite element method to be applied in unbounded domains and cracked domains. The circular artificial boundary was used for solving the exterior elliptic PDEs in early years [Han and Wu (1985); Yu (1985); Han and Bao (2000)] and was generalized later to other artificial boundaries, such as the ellipse, the strip and the ellipsoid to reduce computational costs and enhance numerical results [Ben-Porat and Givoli (1995); Han and Bao (2000); Yu and Jia (2002); Huang, Liu and Yu (2009)].

Yu (1985) obtained the error estimate depended on the radius of the circular artificial boundary and the number of terms after truncating from the infinite series in the integral for solving a harmonic equation. Han and Bao (2000) obtained error estimates for linear elliptic problems outside circular obstacles and in semi-infinite strips. Huang, Liu and Yu (2009) presented a general ellipsoidal artificial boundary method for three dimensional exterior Poisson problems and obtained the error estimate depended on the mesh parameter, the number of terms used in the exact artificial boundary condition, and the location of the artificial boundary.

In this paper, we investigate the coupling method of the finite element and the natural boundary element using an elliptic artificial boundary for exterior anisotropic problems in Section 2, deduce a new error estimate that depends on the mesh size, the location of the elliptic artificial boundary, the number of terms after truncating from the infinite series in the integral in Section 3, and present numerical examples to demonstrate its effectiveness and properties in Section 4, and finally make conclusions in Section 5.

2 The coupling variational problem and its discretization

Consider to solve the following exterior boundary value problem of the anisotropic elliptic partial differential equations with constant coefficients:

$$\begin{cases} a \frac{\partial^2 u}{\partial x^2} + b \frac{\partial^2 u}{\partial y^2} = f, & \text{in } \Omega, \\ u = u_0, & \text{on } \Gamma_0, \end{cases} \quad (1)$$

where Γ_0 is a simple, smooth closed curve surrounding the origin in \mathfrak{R}^2 , Ω is the unbounded domain outside Γ_0 , f has compact support in Ω , $u_0 \in H^{\frac{1}{2}}(\Gamma_0)$, and u satisfies the appropriate boundary conditions at infinity. By making an ellip-

tic artificial boundary curve $\Gamma_1 = \{(x, y) | \alpha x^2 + \beta y^2 = R^2\}$ ($b\beta > a\alpha > 0$) to enclose Γ_0 and the support of f , the area Ω is divided into two subdomains, namely the bounded subdomain Ω_1 surrounded by Γ_0 and Γ_1 , and the unbounded subdomain Ω_2 outside Γ_1 . By the variable transform, $x = \sqrt{a}\xi, y = \sqrt{b}\eta$, the equation becomes a harmonic equation in $\tilde{\Omega}$ and the elliptic artificial boundary becomes $\tilde{\Gamma}_1 = \{(\xi, \eta) | a\alpha\xi^2 + b\beta\eta^2 = R^2\}$.

By introducing elliptic coordinates $(\mu, \phi): \xi = f_0 \cosh \mu \cos \phi, \eta = f_0 \sinh \mu \sin \phi$, which gives confocal ellipses for $\mu > \mu_1$ with common foci $(\pm f_0, 0)$ and $\tilde{\Gamma}_1 = \{(\mu, \phi) | \mu = \mu_1, \phi \in [0, 2\pi]\}$, where $f_0 = \sqrt{\frac{b\beta - a\alpha}{a\alpha b\beta}}R$ and $\mu_1 = \ln \frac{\sqrt{a\alpha} + \sqrt{b\beta}}{\sqrt{b\beta - a\alpha}}$, and by the natural boundary reduction on $\tilde{\Gamma}_1$ [Yu and Jia (2002)], we have the Poisson formula

$$u(\mu, \theta) = \frac{e^{2\mu} - e^{2\mu_1}}{2\pi} \int_0^{2\pi} \frac{u(\mu_1, \theta')}{e^{2\mu} + e^{2\mu_1} - 2e^{\mu+\mu_1} \cos(\theta - \theta')} d\theta',$$

and the natural boundary integral equation

$$\frac{\partial u}{\partial n} = -\frac{1}{\sqrt{J}} \int_0^{2\pi} \frac{1}{4\pi \sin^2 \frac{\theta - \theta'}{2}} u(\mu_1, \theta') d\theta',$$

where $\vec{n} = (n_\xi, n_\eta)$ be the outward normal vector to $\tilde{\Gamma}_1, J = \frac{\alpha \cos^2 \theta + \beta \sin^2 \theta}{a\alpha b\beta} R^2$, and

$$-\frac{1}{4\pi \sin^2 \frac{\theta}{2}} = \frac{1}{2\pi} \sum_{-\infty}^{+\infty} |n| e^{in\theta} = \frac{1}{\pi} \sum_{n=1}^{+\infty} n \cos n\theta.$$

It can be inferred from the Green formula that to find the solution of the problem (1) is equivalent to solve the following variational problem:

$$\begin{cases} \text{find } u \in \hat{H}^1(\tilde{\Omega}_1), \text{ such that} \\ D_1(u, v) + \tilde{D}_2(u, v) = f(v), \forall v \in H_0^1(\tilde{\Omega}_1), \end{cases} \quad (2)$$

where

$$\hat{H}^1(\tilde{\Omega}_1) = \{v \in H^1(\tilde{\Omega}_1) | v|_{\tilde{\Gamma}_0} = u_0\},$$

$$H_0^1(\tilde{\Omega}_1) = \{v \in H^1(\tilde{\Omega}_1) | v|_{\tilde{\Gamma}_0} = 0\},$$

$$D_1(u, v) = \iint_{\Omega_1} (au_x v_x + bu_y v_y) dx dy = \sqrt{ab} \iint_{\tilde{\Omega}_1} (u_\xi v_\xi + u_\eta v_\eta) d\xi d\eta,$$

$$\tilde{D}_2(u, v) = \frac{\sqrt{ab}}{\pi} \int_0^{2\pi} \int_0^{2\pi} \sum_{n=1}^{+\infty} n \cos n(\theta - \theta') u(\mu_1, \theta') v(\mu_1, \theta) d\theta' d\theta$$

for

$$ds = \sqrt{\frac{\alpha \cos^2 \theta + \beta \sin^2 \theta}{\alpha\beta}} R d\theta$$

$$f(v) = \iint_{\Omega_1} f v dx dy = \sqrt{ab} \iint_{\tilde{\Omega}_1} f v d\xi d\eta,$$

The infinite series in the above integral need to be truncated by finite terms in practice. Thus, by using the approximate integral boundary condition, the variational problem (2) is approximated by the approximate variational problem as follows:

$$\begin{cases} \text{find } u^N \in \widehat{H}^1(\tilde{\Omega}_1), \text{ such that} \\ D_1(u^N, v) + \widetilde{D}_2^N(u^N, v) = f(v), \forall v \in H_0^1(\tilde{\Omega}_1), \end{cases} \quad (3)$$

where $\widetilde{D}_2^N(u^N, v) = \frac{\sqrt{ab}}{\pi} \int_0^{2\pi} \int_0^{2\pi} \sum_{n=1}^N n \cos n(\theta - \theta') u^N(\mu_1, \theta') v(\mu_1, \theta) d\theta' d\theta$.

Moreover, by discretizing the approximate variational problem (3), we have discrete approximate variational problem as follows:

$$\begin{cases} \text{find } u_h^N \in \widehat{S}_h(\tilde{\Omega}_1), \text{ such that} \\ D_1(u_h^N, v) + \widetilde{D}_2^N(u_h^N, v) = f(v), \forall v \in S_{0,h}(\tilde{\Omega}_1), \end{cases} \quad (4)$$

where $\widehat{S}_h(\tilde{\Omega}_1) = \{v \in S_h(\tilde{\Omega}_1) | v|_{\tilde{\Gamma}_0} = u_0\}$, $S_{0,h}(\tilde{\Omega}_1) = \{v \in S_h(\tilde{\Omega}_1) | v|_{\tilde{\Gamma}_0} = 0\}$, piecewise linear functions on domain $\tilde{\Omega}_1$ are chosen as the basis functions such that $S_h(\tilde{\Omega}_1) \subset H^1(\tilde{\Omega}_1)$ is the finite element solution space on $\tilde{\Omega}_1$. Let the nodes on the elliptic artificial boundary $\tilde{\Gamma}_1$ be equally distributed by $\phi_i = \frac{2\pi i}{N}$ ($i = 0, 1, \dots, \bar{N}$) in the elliptic coordinates. Then linear algebraic equations $QU = F$ can be obtained by the discrete variational problem (4), where $Q = Q_1 + Q_2$, Q_1 is from bilinear form $D_1(\cdot, \cdot)$ and Q_2 is from $\widetilde{D}_2^N(\cdot, \cdot)$. Specifically speaking, Q_1 can be derived by the finite element method, the non-zero sub-matrix $Q_2 = \sqrt{ab}[q_{ij}]_{\bar{N} \times \bar{N}}$, and $q_{ij} = \frac{4\bar{N}^2}{\pi^3} \sum_{n=1}^{\infty} \frac{1}{n} \sin^4 \frac{n\pi}{\bar{N}} \cos \frac{2n(i-j)\pi}{\bar{N}}$ is the natural boundary element stiffness matrix on $\tilde{\Gamma}_1$, and F can be derived by u_0 and f .

3 The error analysis

Denoting u , u^N and u_h^N the solutions of variational problem (2), (3) and (4) respectively, and $u_1 = u|_{\tilde{\Gamma}_1}$ and $v_1 = v|_{\tilde{\Gamma}_1}$, we prove the existence and uniqueness of these solutions and derive the error estimate between the discrete solution u_h^N and the exact solution u in this section.

Lemma 1. $\widetilde{D}_2(u_1, v_1)$ and $\widetilde{D}_2^N(u_1, v_1)$ are both a semi-definite symmetric and continuous bilinear form on $H^{\frac{1}{2}}(\tilde{\Gamma}_1)$.

Proof. Let $u_1 = \sum_{n=-\infty}^{+\infty} a_n e^{in\theta}$, $a_{-n} = \bar{a}_n$, $v_1 = \sum_{n=-\infty}^{+\infty} b_n e^{in\theta}$, $b_{-n} = \bar{b}_n$, $n = 0, 1, 2, \dots$, we have

$$\begin{aligned} \tilde{D}_2(u_1, v_1) &= \sqrt{ab} \int_0^{2\pi} \sum_{n=-\infty}^{+\infty} |n| a_n e^{in\theta} \sum_{m=-\infty}^{+\infty} b_m e^{im\theta} d\theta = 2\pi\sqrt{ab} \sum_{n=-\infty}^{+\infty} |n| a_n \bar{b}_n, \\ |\tilde{D}_2(u_1, v_1)| &= 2\pi\sqrt{ab} \left(\sum_{n=-\infty}^{+\infty} |n| |a_n|^2 \right)^{\frac{1}{2}} \times \left(\sum_{n=-\infty}^{+\infty} |n| |b_n|^2 \right)^{\frac{1}{2}} \\ &\leq 2\pi\sqrt{ab} \left(\sum_{n=-\infty}^{+\infty} (1+n^2)^{\frac{1}{2}} |a_n|^2 \right)^{\frac{1}{2}} \left(\sum_{n=-\infty}^{+\infty} (1+n^2)^{\frac{1}{2}} |b_n|^2 \right)^{\frac{1}{2}} \\ &= 2\pi\sqrt{ab} \|u_1\|_{\frac{1}{2}, \tilde{\Gamma}_1} \|v_1\|_{\frac{1}{2}, \tilde{\Gamma}_1}. \end{aligned}$$

In the same way, we can get

$$|\tilde{D}_2^N(u_1, v_1)| = |2\pi\sqrt{ab} \sum_{n=-N}^N |n| a_n \bar{b}_n| \leq 2\pi\sqrt{ab} \|u_1\|_{\frac{1}{2}, \tilde{\Gamma}_1} \|v_1\|_{\frac{1}{2}, \tilde{\Gamma}_1},$$

$$\tilde{D}_2(u_1, u_1) = 2\pi\sqrt{ab} \sum_{n=-\infty}^{+\infty} |n| |a_n|^2 \geq 0 \text{ and } \tilde{D}_2^N(u_1, u_1) = 2\pi\sqrt{ab} \sum_{n=-N}^N |n| |a_n|^2 \geq 0. \quad \square$$

It is easy to see the continuity on $H^{\frac{1}{2}}(\tilde{\Gamma}_1)$ can be further enhanced to $H^{\frac{1}{2}}(\tilde{\Gamma}_1)/P_0$. In addition,

$$\begin{aligned} \tilde{D}_2(u_1, u_1) &= 2\pi\sqrt{ab} \sum_{n=-\infty}^{+\infty} |n| |a_n|^2 \geq \pi\sqrt{2ab} \sum_{-\infty, n \neq 0}^{+\infty} (1+n^2)^{\frac{1}{2}} |a_n|^2 \\ &= \pi\sqrt{2ab} \|u_1\|_{H^{\frac{1}{2}}(\tilde{\Gamma}_1)/P_0}^2. \end{aligned}$$

That is to say $\tilde{D}_2(u_1, v_1)$ is V -elliptic on $H^{\frac{1}{2}}(\tilde{\Gamma}_1)/P_0$.

Theorem 1. The variational problem (2) and the approximate variational problem (3) have a unique solution on $H^1(\tilde{\Omega}_1)$, respectively.

Proof. By the properties of $D_1(u, v)$ and Lemma 1, we know that both $D_1(u, v) + \tilde{D}_2(u_1, v_1)$ and $D_1(u, v) + \tilde{D}_2^N(u_1, v_1)$ are symmetric and continuous V -elliptic bilinear forms on $H^1(\tilde{\Omega}_1)$. In addition, note that $f(v)$ is a continuous linear function on $H^1(\tilde{\Omega}_1)$. Then we can prove this theorem by the *Lax – Milgram* theorem. \square

Similarly, we have

Theorem 2. The discrete approximate variational problem (4) has a unique solution $u_h^N \in S_h(\tilde{\Omega}_1)$. \square

Lemma 2. There exists a constant C independent of h and N for the solution u_h^N , such that

$$\|u - u_h^N\|_{1, \tilde{\Omega}_1} \leq C \left\{ \inf_{v \in S_h(\tilde{\Omega}_1)} \|u - v\|_{1, \tilde{\Omega}_1} + \sup_{v_1 \in S_{0,h}(\tilde{\Omega}_1)} \frac{|\tilde{D}_2^N(u_1, v_1) - \tilde{D}_2(u_1, v_1)|}{\|v_1\|_{1, \tilde{\Omega}_1}} \right\}.$$

(5)

Proof. Equality $D_1(u, v) + \tilde{D}_2(u, v) = f(v)$ of variational problem (2) can be written as

$$D_1(u, v) + \tilde{D}_2^N(u, v) = \tilde{D}_2^N(u, v) - \tilde{D}_2(u, v) + f(v), \forall v \in H_0^1(\tilde{\Omega}_1).$$

Subtracting the equality $D_1(u_h^N, v) + \tilde{D}_2^N(u_h^N, v) = f(v)$ of variational problem (4) from the above, we obtain

$$D_1(u - u_h^N, v) + \tilde{D}_2^N(u - u_h^N, v) = \tilde{D}_2^N(u, v) - \tilde{D}_2(u, v), \forall v \in S_{0,h}(\tilde{\Omega}_1).$$

For $\forall v \in \hat{S}_h(\tilde{\Omega}_1)$, since $u_h^N - v \in S_{0,h}(\tilde{\Omega}_1)$, we have

$$\begin{aligned} \|u_h^N - v\|_{1,\tilde{\Omega}_1}^2 &\leq C[D_1(u_h^N - v, u_h^N - v) + \tilde{D}_2^N(u_h^N - v, u_h^N - v)] \\ &= C[D_1(u - v, u_h^N - v) + \tilde{D}_2^N(u - v, u_h^N - v) + \tilde{D}_2(u, u_h^N - v) - \tilde{D}_2^N(u, u_h^N - v)] \\ &\leq C[\|u - v\|_{1,\tilde{\Omega}_1} \|u_h^N - v\|_{1,\tilde{\Omega}_1} + |\tilde{D}_2(u, u_h^N - v) - \tilde{D}_2^N(u, u_h^N - v)|]. \end{aligned}$$

Therefore,

$$\|u_h^N - v\|_{1,\tilde{\Omega}_1} \leq C\{\|u - v\|_{1,\tilde{\Omega}_1} + \sup_{v_1 \in S_{0,h}(\tilde{\Omega}_1)} \frac{|\tilde{D}_2^N(u_1, v_1) - \tilde{D}_2(u_1, v_1)|}{\|v_1\|_{1,\tilde{\Omega}_1}}\}.$$

The proof follows by the triangle inequality $\|u - u_h^N\|_{1,\tilde{\Omega}_1} \leq \|u - v\|_{1,\tilde{\Omega}_1} + \|u_h^N - v\|_{1,\tilde{\Omega}_1}$. \square

Theorem 3. For the problems (2) and (4), if $u \in H^2(\tilde{\Omega}_1) \cap H^{k-\frac{1}{2}}(\tilde{\Gamma}_1)$, $k = 2, 3, \dots$, then

$$\|u - u_h^N\|_{1,\tilde{\Omega}_1} \leq C\{h \|u\|_{2,\tilde{\Omega}_1} + \frac{1}{N^{k-1}} \|u_1\|_{k-\frac{1}{2},\tilde{\Gamma}_1}\}. \tag{6}$$

Moreover, if $\tilde{\Gamma}_0 = \{(\bar{\mu}_0, \phi) | \bar{\mu}_0 < \mu_1, \phi \in [0, 2\pi]\}$ be the smallest ellipse to enclose the support of f , then

$$\|u - u_h^N\|_{1,\tilde{\Omega}_1} \leq C\{h \|u\|_{2,\tilde{\Omega}_1} + \frac{1}{N^{k-1} e^{(N+1)(\mu_1 - \bar{\mu}_0)}} \|u\|_{k-\frac{1}{2},\tilde{\Gamma}_0}\}, \tag{7}$$

where C is a constant independent of h and N .

Proof. By Lemma 2, for the first term, we have

$$\inf_{v \in \hat{S}_h(\tilde{\Omega}_1)} \|u - v\|_{1,\tilde{\Omega}_1} \leq Ch \|u\|_{2,\tilde{\Omega}_1}.$$

For the second term, we have

$$\begin{aligned} &|\tilde{D}_2^N(u_1, v_1) - \tilde{D}_2(u_1, v_1)| \\ &= |2\pi\sqrt{ab} \sum_{|n| \geq N+1}^{+\infty} |n| a_n \bar{b}_n| \leq \frac{2\pi\sqrt{ab}}{N^{k-1}} |\sum_{|n| \geq N+1}^{+\infty} |n|^k a_n \bar{b}_n| \\ &\leq \frac{2\pi\sqrt{ab}}{N^{k-1}} [\sum_{|n| \geq N+1}^{+\infty} (n^2 + 1)^{k-\frac{1}{2}} |a_n|^2]^{\frac{1}{2}} [\sum_{|n| \geq N+1}^{+\infty} (n^2 + 1)^{k-\frac{1}{2}} |b_n|^2]^{\frac{1}{2}} \\ &\leq \frac{2\pi\sqrt{ab}}{N^{k-1}} \|u_1\|_{k-\frac{1}{2},\tilde{\Gamma}_1} \|v_1\|_{\frac{1}{2},\tilde{\Gamma}_1}. \end{aligned}$$

So, the estimate (6) holds, since by the trace theorem we have

$$|\tilde{D}_2^N(u_1, v_1) - \tilde{D}_2(u_1, v_1)| \leq \frac{2\pi\sqrt{ab}}{N^{k-1}} \|u_1\|_{k-\frac{1}{2}, \tilde{\Gamma}_1} \|v_1\|_{1, \tilde{\Omega}_1}.$$

Moreover, we have

$$\begin{aligned} u(\mu, \phi) &= \frac{e^{2\mu} - e^{2\bar{\mu}_0}}{2\pi} \int_0^{2\pi} \frac{u(\bar{\mu}_0, \phi')}{e^{2\mu} + e^{2\bar{\mu}_0} - 2e^{\mu+\bar{\mu}_0} \cos(\phi-\phi')} d\phi' \\ &= \frac{1}{2\pi} \sum_{n=-\infty}^{+\infty} \int_0^{2\pi} e^{-|n|(\mu-\bar{\mu}_0)} e^{in(\phi-\phi')} \sum_{m=-\infty}^{+\infty} a_m e^{im\phi'} d\phi' \\ &= \sum_{n=-\infty}^{+\infty} e^{-|n|(\mu-\bar{\mu}_0)} e^{in\phi} \sum_{m=-\infty}^{+\infty} a_m \frac{1}{2\pi} \int_0^{2\pi} e^{i(m-n)\phi'} d\phi' \\ &= \sum_{n=-\infty}^{+\infty} a_n e^{-|n|(\mu-\bar{\mu}_0)} e^{in\phi}, \quad \mu > \bar{\mu}_0, \end{aligned}$$

where $u(\bar{\mu}_0, \phi') = \sum_{m=-\infty}^{+\infty} a_m e^{im\phi'}$, $a_{-m} = \bar{a}_m$, $m = 0, 1, 2, \dots$. Therefore,

$$u_1 = u(\mu_1, \phi) = \sum_{n=-\infty}^{+\infty} a_n e^{-|n|(\mu_1-\bar{\mu}_0)} e^{in\phi}.$$

Finally, we obtain

$$\begin{aligned} |\tilde{D}_2^N(u_1, v_1) - \tilde{D}_2(u_1, v_1)| &= |2\pi\sqrt{ab} \sum_{|n| \geq N+1}^{+\infty} |n| a_n e^{-|n|(\mu_1-\bar{\mu}_0)} \bar{b}_n| \\ &\leq \frac{2\pi\sqrt{ab}}{N^{k-1} e^{(N+1)(\mu_1-\bar{\mu}_0)}} \left| \sum_{|n| \geq N+1}^{+\infty} |n|^k a_n \bar{b}_n \right| \\ &\leq \frac{2\pi\sqrt{ab}}{N^{k-1} e^{(N+1)(\mu_1-\bar{\mu}_0)}} \|u\|_{k-\frac{1}{2}, \tilde{\Gamma}_0} \|v_1\|_{1, \tilde{\Omega}_1}. \end{aligned}$$

So, the estimate (7) follows. \square

4 Numerical Examples

Numerical experiments of the coupling method and its error estimate with the natural boundary reduction on an ellipse for solving exterior anisotropic problems are demonstrated as the following.

Example 1. We consider the exterior anisotropic problem:

$$\begin{cases} \varepsilon \frac{\partial^2 u}{\partial x^2} + \frac{\partial^2 u}{\partial y^2} = 0, & \text{in } \Omega, \\ u = u_0, & \text{on } \Gamma_0, \end{cases}$$

where Ω is an exterior domain with the elliptic inner boundary $\Gamma_0 = \{(x, y) \mid \frac{x^2}{3} + y^2 = 1\}$. By using coordinate transformation $x = \sqrt{\varepsilon}\xi$ and $y = \eta$, we turn the original problem into the problem as the following:

$$\begin{cases} \Delta u = 0, & \text{in } \tilde{\Omega}, \\ u = u_0, & \text{on } \tilde{\Gamma}_0, \end{cases}$$

where $\tilde{\Gamma}_0 = \{(\mu_0, \phi) | \mu_0 = \ln \frac{1 + \sqrt{\varepsilon/3}}{\sqrt{1 - \varepsilon/3}}, \phi \in [0, 2\pi]\}$. If $\varphi(z) = \frac{1}{z}$, then $u(x, y) = \text{Re}\varphi(\frac{x}{\sqrt{\varepsilon}} + iy)$ is the exact solution of original problem and $u_0 = u|_{\tilde{\Gamma}_0}$. Take the confocal elliptic artificial boundary $\tilde{\Gamma}_1 = \{(\mu_1, \phi) | \mu_1 = 2.5\mu_0, \phi \in [0, 2\pi]\}$. Make the partition $\tilde{\Omega}_{1,h}$ with $\varepsilon = 0.5$ as shown in Figure 1. The numerical results for different mesh sizes h and coefficients ε are shown in Table 1, for different truncation term numbers N are shown in Figure 2.

Table 1: The maximum error on $\Gamma_{1,h/m}$ with $N = 20$ for $m=1, 2, 4, 8, 16$

mesh	$\varepsilon = 1$	ratio	$\varepsilon = 0.5$	ratio	$\varepsilon = 0.05$	ratio
h	0.0544		0.0370		0.0041	
$h/2$	0.0167	3.2574	0.0169	2.1893	0.0035	1.1714
$h/4$	0.0040	4.1750	0.0041	4.1219	0.0016	2.1875
$h/8$	0.0010	4.0000	0.0010	4.1000	5.1101e-04	3.1311
$h/16$	2.5503e-04	3.9211	2.5111e-04	3.9823	1.2758e-04	4.0054

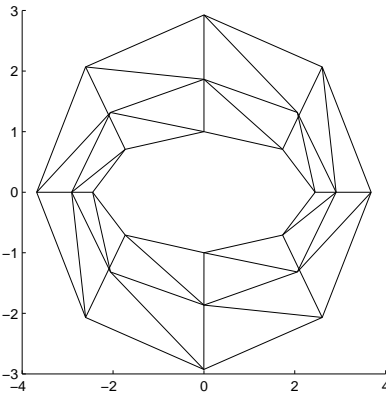


Figure 1: $\tilde{\Omega}_{1,h}$ with $\varepsilon = 0.5$ and $\mu_1 = 2.5\mu_0$.

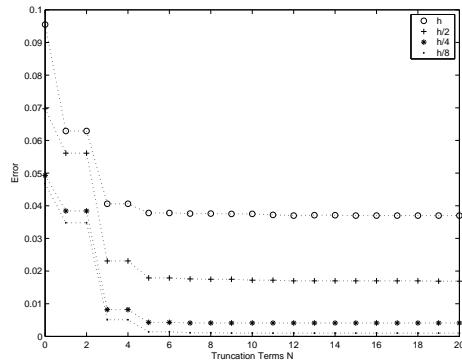


Figure 2: $|u - u_{h/m}^N|_{\infty, \Gamma_{1,h/m}}$ w. r. t. N and m .

Example 2. Assume in Example 1 that $\varphi(z) = \frac{1}{z^3}$, then the corresponding numerical results are shown in Table 2 and Figure 3.

Table 2: Maximum error on $\Gamma_{1,h/m}$ with $N = 20$ for $m=1, 2, 4, 8, 16$

mesh	$\varepsilon = 1$	ratio	$\varepsilon = 0.5$	ratio	$\varepsilon = 0.05$	ratio
h	0.0608		0.0458		0.0024	
$h/2$	0.0322	1.8882	0.0127	3.6063	0.0037	2.2703
$h/4$	0.0089	3.6180	0.0057	2.2281	0.0024	1.5417
$h/8$	0.0023	3.8696	0.0012	4.7500	2.1156e-04	11.3443
$h/16$	5.5542e-04	4.1410	3.1349e-04	3.8279	1.9761e-05	10.7059

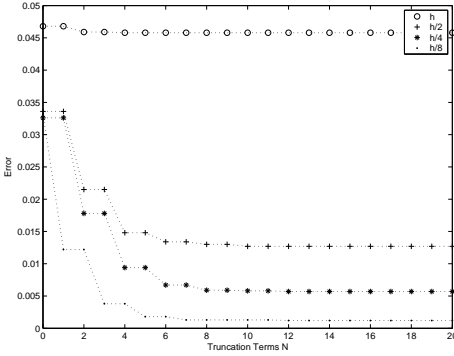


Figure 3: The error in Ex. 2 w.r.t. h and N .

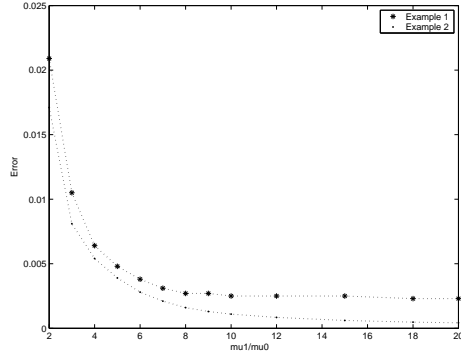


Figure 4: The error on $\mu = 2.5\mu_0$ w.r.t. μ_1 .

The maximum errors on $\mu = 2.5\mu_0$ for different location of the artificial boundary in Example 1 and 2 are shown in and Figure 4.

Example 3. Assume in Example 1 that $\tilde{\Gamma}_0$ is a rectangle with center at $(0,0)$, then we have the corresponding results in Table 3 and Figure 5.

Table 3: Maximum error on $\Gamma_{1,h/m}$ with $N = 20$

mesh	$\varepsilon = 1$	ratio	$\varepsilon = 0.5$	ratio	$\varepsilon = 0.05$	ratio
h	0.1041		0.1303		0.1389	
$h/2$	0.0234	4.4487	0.0361	3.6094	0.0740	1.8770
$h/4$	0.0061	3.8360	0.0082	4.4024	0.0423	1.7494
$h/8$	0.0015	4.0667	0.0020	4.1000	0.0171	2.4737
$h/16$	3.8447e-04	3.9014	4.9386e-04	4.0497	0.0096	1.7813

Example 4. Assume in Example 2 that $\tilde{\Gamma}_0$ is a rectangle with center at $(0,0)$, then we have the corresponding results in Table 4 and Figure 6.

Table 4: Maximum error on $\Gamma_{1,h/m}$ with $N = 20$

mesh	$\varepsilon = 1$	ratio	$\varepsilon = 0.5$	ratio
h	0.0460		0.0335	
$h/2$	0.0180	2.5556	0.0243	1.3786
$h/4$	0.0054	3.3333	0.0063	3.8571
$h/8$	0.0016	3.3750	0.0016	3.9375
$h/16$	4.1899e-04	3.8187	4.1505e-04	3.8549

5 Conclusions

We discuss the coupling method with the natural boundary reduction on an elliptic artificial boundary for solving exterior anisotropic problems, obtain its appropriate a priori estimate and demonstrate the numerical experiments in this paper. The

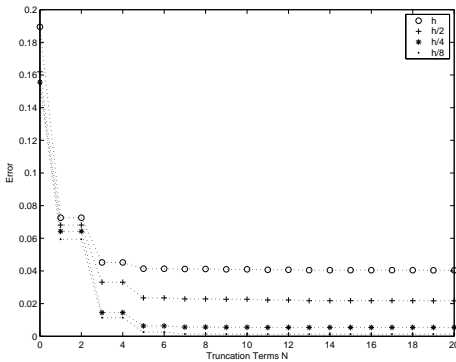


Figure 5: The error in Ex. 3 w.r.t. h and N .

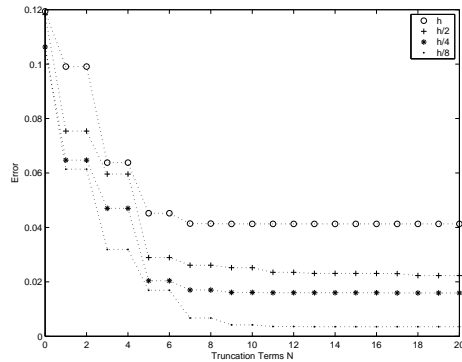


Figure 6: The error in Ex. 4 w.r.t. h and N .

coupling method can be accomplished conveniently by coupling directly the stiffness matrix of FEM and the stiffness matrix of natural BEM. This natural coupling method is effective and its error estimate is verified, too. We can see that: 1) the error decreases greatly while the truncation term number N increases in the beginning and does not decrease too much later on; 2) the error also depends on the location of the artificial boundary in a similar way; 3) the error mainly comes from the mesh size h and is roughly of order $O(h^2)$ when N is already not too small and the location of the artificial boundary is not too nearby, and even if the ratio of coefficients is very small, only the constant in the error estimate increases. Thus, it is inadvisable to increase the truncation term number N and the distant between the artificial boundary and the inner boundary Γ_0 too much in order to reduce the error, because in that way the computational cost from the larger computational domain becomes much higher but the error decreases very less. The error is formed by two items, one is polynomially from the approximation using FEM, the other is geometrically from a multiplication of two factors about the truncation and the location. Comparing the three factors, the main burden to reduce the error comes from FEM for the small mesh size h . But fortunately, the bounded subdomain of FEM is now confined small enough.

References

- Ben-Porat G.; Givoli D.** (1995): Solution of unbounded domain problems using elliptic artificial boundaries. *Commun. Numer. Meth. Eng.*, vol. 11, pp. 735-741.
- Delfim Jr. S.** (2008): A time-domain fem-bem iterative coupling algorithm to numerically model the propagation of electromagnetic waves. *CMES: Computer Modeling in Engineering & Sciences*, vol. 32, pp. 57-68.

- Enquist B.; Majda A.** (1977): Absorbing boundary conditions for numerical simulation of waves. *Math. Comput.*, vol. 31, pp. 629-651.
- Feng K.** (1983): Finite element method and natural boundary reduction. *Proc. of Inter. Cong. of Math.*, Warszawa, pp. 1439-1453.
- Feng K.; Yu D.-H.** (1983): Canonical integral equations of elliptic boundary value problems and their numerical solutions. *Proc. of China-France Symposium on the Finite Element Method* (Feng, K. and Lions, J. L. ed.), Science Press and Gordon Breach, Beijing, New York, pp. 211-252.
- Givoli D.** (1992): *Numerical Methods for Problems in Infinite Domains*. Elsevier, Amsterdam.
- Han H.; Bao W.** (2000): Error Estimates for the Finite Element Approximation of Problems in Unbounded Domains. *SIAM J. Numer. Anal.*, vol. 37, pp. 1101-1119.
- Han H.; Wu X.** (1985): Approximation of infinite boundary condition and its application to finite element method. *J. Comput. Math.*, vol. 3, pp. 179-192.
- Huang H.-Y.; Liu D.-J.; Yu D.-H.** (2009): Solution of exterior problem using ellipsoidal artificial boundary. *J. Comput. Appl. Math.*, Vol. 231, pp. 434-446.
- Johnson C.; Nedelec J. C.** (1980): On the coupling of boundary integral and finite element methods. *Math. Comput.*, vol. 35, pp. 1063-1079.
- Keller J. B.; Givoli D.** (1989): An exact non-reflection boundary conditions. *J. Comput. Phys.*, vol. 82, pp. 172-192.
- Koyama D.** (2009): Error estimates of the finite element method for the exterior Helmholtz problem with a modified DtN boundary condition. *J. Comput. Appl. Math.*, vol. 232, pp. 109-121.
- Ying L. A.** (2006): *Numerical Methods for Exterior Problems*. World Scientific, New Jersey.
- Yu D.-H.** (2002): *Natural Boundary Integral Method and Its Applications*. Kluwer Academic Publisher/Science Press, Beijing, Dordrecht, New York, London.
- Yu D.-H.** (1985): Approximation of boundary conditions at infinity for a harmonic equation. *J. Comput. Math.*, vol. 3, pp. 219-227.
- Yu D.-H.; Huang H.-Y.** (2008): The artificial boundary method for a nonlinear interface problem on unbounded domain. *CMES: Computer Modeling in Engineering & Sciences*, vol. 35, pp.227-252.
- Yu D.-H.; Jia Z.-P.** (2002): Natural integral operator on elliptic boundary and the coupling method for an anisotropic problem. *Math. Numer. Sinica*, vol. 24, pp. 375-384; *China J. Numer. Math. Appl.*, vol. 24, 95-107.

